

# Optical profilometry for forensic bloodstain imaging

Theresa Stotesbury<sup>1</sup>, Brayden Vale<sup>1</sup>, Amanda Orr<sup>2</sup>, and Colin Elliott<sup>1</sup>

<sup>1</sup>University of Ontario Institute of Technology Faculty of Science

<sup>2</sup>Trent University

January 9, 2023

## Abstract

Understanding the physical, chemical and biological changes that occur during the drying of a bloodstain is important in many aspects of forensic science including bloodstain pattern analysis and time since deposition estimation. This research assesses the use of optical profilometry to analyze changes in the surface morphology of degrading bloodstains created using three different volumes (4, 11, and 20  $\mu\text{L}$ ) up to four weeks after deposition. We analyzed six surface characteristics, including surface average roughness, kurtosis, skewness, maximum height, number of cracks and pits, and height distributions from the topographical scans obtained from bloodstains. Full and partial optical profiles were obtained to examine long-term (minimum of 1.5 hour intervals) and short-term (5 minute intervals) changes. The majority of the changes in surface characteristics occurred within the first 35 minutes after bloodstain deposition, in agreement with current research in bloodstain drying. Optical profilometry is a non-destructive and efficient method to obtain surface profiles of bloodstains, and can be integrated easily into additional research workflows including but not limited to time since deposition estimation.

## Optical profilometry for forensic bloodstain imaging

Brayden Vale<sup>a</sup>, Amanda Orr<sup>b</sup>, Colin Elliott<sup>c</sup>, Theresa Stotesbury<sup>d\*</sup>

\*Corresponding author: *theresa.stotesbury@ontariotechu.ca*

<sup>a</sup> Forensic Science Undergraduate Program, Ontario Tech University, 2000 Simcoe St N, Oshawa, ON, Canada, L1G 0C5

<sup>b</sup> Environmental and Life Sciences Graduate Program, Trent University, 1600 West Bank Drive, Peterborough, ON, Canada, K9J 0G2

<sup>c</sup> Applied Bioscience Graduate Program, Faculty of Science, Ontario Tech University, 2000 Simcoe St N, Oshawa, ON, Canada, L1G 0C5

<sup>d</sup> Faculty of Science, Forensic Science, Ontario Tech University, 2000 Simcoe St N, Oshawa, ON, Canada, L1G 0C5

**ORCID:** AO (0000-0002-2245-8448); CE (0000-0001-5883-0291); TE (0000-0001-6452-4389)

**Data Availability Statement:** Scans are available by request and data is available through <https://gitlab.com/f4301/bloodstain-profilometry>.

**Funding Statement:** We are thankful for the funding support to conduct this research. This work was supported by the Natural Sciences and Engineering Research Council of Canada (NSERC) Discovery and Discovery Accelerator Supplement Grants (RGPIN-2020-05816) awarded to TS. Authors CE and AO are supported through the NSERC Canada Graduate CGS-M (MSc) and CGS-D (PhD) Scholarship programs respectively.

**Conflict of Interest Disclosure:** The authors have no conflicts of interests to declare.

**Acknowledgements:** The authors would like to formally acknowledge Mitchell Tiessen, Kgalalelo Rampete, Julia Harvey, Dhrumik Patel, and Laurianne Lagace, who assisted BV with fluid property measurements throughout his undergraduate thesis. A most special thank-you goes to Dr. Iraklii Ebralidze, of the Ontario Tech University Materials Characterization Facility for training BV on the optical profilometer.

**Abstract:**

Understanding the physical, chemical and biological changes that occur during the drying of a bloodstain is important in many aspects of forensic science including bloodstain pattern analysis and time since deposition estimation. This research assesses the use of optical profilometry to analyze changes in the surface morphology of degrading bloodstains created using three different volumes (4, 11, and 20  $\mu\text{L}$ ) up to four weeks after deposition. We analyzed six surface characteristics, including surface average roughness, kurtosis, skewness, maximum height, number of cracks and pits, and height distributions from the topographical scans obtained from bloodstains. Full and partial optical profiles were obtained to examine long-term (minimum of 1.5 hour intervals) and short-term (5 minute intervals) changes. The majority of the changes in surface characteristics occurred within the first 35 minutes after bloodstain deposition, in agreement with current research in bloodstain drying. Optical profilometry is a non-destructive and efficient method to obtain surface profiles of bloodstains, and can be integrated easily into additional research workflows including but not limited to time since deposition estimation.

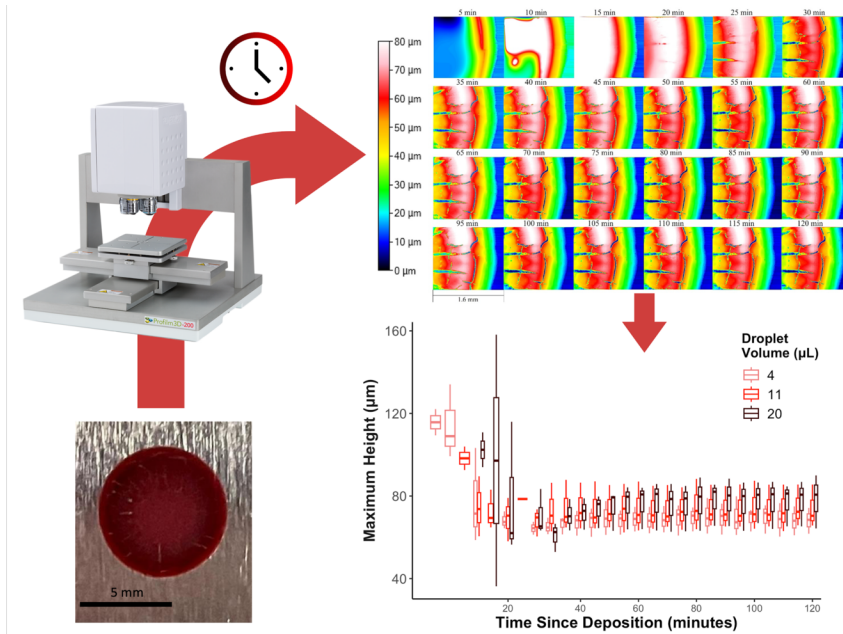
**Keywords:**

Drying bloodstains, surface profile, time since deposition (TSD), forensic science, crack formation

**Research Highlights:**

- Optical profilometry is a non-contact tool to scan bloodstains in ambient conditions
- Drying phases are observable in small drip bloodstains
- Significant surface morphology changes occur within 35 minutes after deposition

**Graphical Abstract:**



## 1. Introduction

Blood is a versatile type of evidence in forensic science investigations and can provide important information, such as the ‘who’, ‘what’, and ‘how’ as it relates to criminal investigations. For example, blood can be collected and used for DNA analysis, chemically analyzed to identify drugs and other substances, and physically observed to conduct bloodstain pattern analysis (BPA) [1,2]. Whole blood is composed of red blood cells (RBCs), white blood cells (WBCs) – which contain DNA, and platelets, all suspended in a liquid plasma [3]. Blood is a non-Newtonian and shear-thinning fluid, meaning its viscosity is dependent on the amount of applied shear stress, which causes blood to become more liquid-like at higher shear rates [4]. Bloodstains observed at crime scenes display a large variability in appearance. For example, their size, shape, distribution and colour are largely dependent on the mechanism, environmental and surface conditions of their deposition and observed degradation state (more commonly referred to as time since deposition, or TSD) [1,5].

The drying process of blood begins immediately after exiting the body [6] and has been summarized in detail by Sobac and Brutin [7] to occur in three phases; the pre-gelation phase (Phase 0), the gelation phase (Phase 1) and the post-gelation phase (Phase 2). In Phase 0, RBCs begin to migrate toward the edge of the bloodstain where a desiccation line begins to form. In Phase 1, a compaction front forms at the edge of the bloodstain and moves inwards toward the center. Simultaneously, the bloodstain desiccates inward, while a dark red ‘donut’ can be seen; this donut is highly concentrated with RBCs and moves from the center of the bloodstain to the outside. The donut begins to desiccate, and the center of the bloodstain turns a lighter red. By this point, the edge of the bloodstain is almost fully desiccated, and the donut shape has become a solid mass; cracks have begun to form at the edge of the bloodstain and propagate inwards. By Phase 2, the center of the bloodstain begins to dry and cracks begin to form, while the rim becomes fully desiccated. The remainder of the bloodstain then becomes desiccated and no further changes are observed. Laan et al. [7] and Benabdelhalim et al. [6] found a similar drying process analyzing blood pools (~4 mL); however, the first phase consisted of the bloodstain coagulating, and increased colour changes were observed, including the pool changing to a black colour as it desiccated.

Droplet desiccation is influenced by a variety of parameters such as packed cell volume (PCV%, the packed cell volume percentage in a blood sample), surface wettability, temperature, and relative humidity (RH) [8]. Larkin et al. [9] investigated the effects of PCV% on the drying process and corroborated the drying

mechanism described by Sobac et al. [10]. In their study, it was found that a decrease in PCV% increased the effects of Marangoni flow due to surface tension differences, but did not influence drying time [9]. RH also plays a key role in the drying process and phase separation of larger bloodstains [6]; as RH increases, the transfer of water between its liquid and gaseous state is limited by the increased concentration of water in the air [11]. This decreased evaporation rate leads to a variation in plaque formation in the rim, which are sections of the rim that separate from the surrounding bloodstain to produce islands of dried blood [11]. Temperature differences also influence the drying time and morphology of bloodstains. Ramsthaller et al. [8] observed an increase in drying times of bloodstains from 30 min (24 °C) to upwards of 120 min (15 °C), and Pal et al. [12] observed sharper-edged rings in bloodstains deposited at greater temperatures (35 and 45 °C) compared to 25 °C.

Degrading bloodstains have been imaged by techniques such as scanning electron microscopy (SEM) [13], atomic force microscopy (AFM) [14,15], and hyperspectral imaging [16,17]. Surface profilometry is a technique used to measure and analyze the topographies of small surfaces. Optical profilometry provides a contact-free measurement using optical sensors, providing detailed topographical information without touching the bloodstain [18]. As a non-destructive technique, optical profilometry has emerged as a useful tool in forensic science analyses. Alcaraz-Fossoul et al. [19] showed that optical profilometry could visualize latent fingerprints without pre-treating them, and in aging studies, fingerprints were not required to be re-developed before each collection point. Heikkinen et al. [20] used white light interferometry to identify similarities and differences between tool mark samples and further identified firing pins via impression details that could not be identified using 2D imaging. Hertaeg et al. [21] used laser confocal microscopy to collect height profiles of bloodstains with varying concentrations of RBCs suspended in three different solutions: plasma, phosphate buffered saline (PBS), and bovine serum albumin (BSA). Their results corroborated previous findings that higher RBC concentrations increase the amount of RBC deposition at the edge of the bloodstain [21]. From this, we asked whether optical profilometry, using full scan and centre profiles, can also be useful in monitoring time-wise changes in degrading bloodstains. We investigated the changes in bloodstain surface characteristics such as surface height, surface roughness, and number of cracks and pits for small drip bloodstains over the course of four weeks. In addition, we evaluated the influence of small differences in bloodstain volume on the extent of these changes.

## 2. Materials and Methods

### 2.1 Blood Source

Whole bovine blood with 12.5% volume by volume (v/v) acid citrate dextrose anticoagulant solution A (ACD-A) was used to create the drip bloodstains. Whole bovine blood from three biological replicates was collected from Windcrest Meat Packers (Port Perry, Ontario, Canada) and mixed with ACD-A. The ACD-A anticoagulant was created by dissolving 0.3072 g of citric acid monohydrate, 0.8448 g of sodium citrate dehydrate, and 0.8550 g of D (+) glucose (Sigma Aldrich, Ontario, Canada) into 62.50 mL of Millipore water. The drip bloodstains were created within 48 hours of blood collection. Fluid properties of the whole blood, including density, surface tension, viscosity, and PCV% were measured in ambient conditions on the same day as the blood collection (see Table S1).

### 2.2 Drip Bloodstain Creation

Two different experiments were completed: long-term and short-term time experiments. For the long-term experiments, three 90° drip bloodstains were created using a 10 µL gas-tight syringe (Hamilton 80300, 701 N) in triplicate 1.5 hours apart from each other. The syringe was held by a retort stand 30 cm above a 15 cm x 15 cm polished aluminum plate. The gas-tight syringe was used to collect 4 µL of blood, which was deposited onto the plate as a single droplet. The syringe was rinsed with MilliQ water and dried between generation of each droplet. For the short-term experiments, three different volumes of blood were investigated: 4 µL, which was deposited by a gas-tight syringe, 11 µL, and 20 µL, both of which were deposited using a micropipette. A gas-tight syringe was used to deposit 4 µL instead of a micropipette because the diameter of the micropipette

tip was too large for the blood to drop without using additional force. All experiments were completed at ambient temperatures ( $22 \pm 2^\circ\text{C}$ ).

### 2.3 Optical Profilometry

Immediately after bloodstain deposition, a Filmetrics Profilm3D Optical Profiler was used to scan the bloodstains. Scans of the bloodstains were taken with a 20x objective lens (1.0 x 0.85 mm field of view) with a 10% overlap to produce a topographic scan through ProFilm 3D. In the long-term experiments, scans were taken of the entire bloodstain, which took approximately 90 minutes. Scans were captured at 1.5 hours, 6 hours, 10.5 hours, 24 hours, 48 hours, 72 hours, 120 hours, 1 week, 2 weeks, 3 weeks, and 4 weeks after deposition. In the short-term experiments, to achieve faster scan times, scans of the right side of the bloodstain were taken. Scans were taken every five minutes up to two hours after deposition; these scans included a portion of the plate, as well as the rim of the bloodstain. For the rim of the bloodstain to be visualized, the scan area was progressively increased as volume increased (from 1.6 mm x 1.6 mm x 80  $\mu\text{m}$  for 4  $\mu\text{L}$ , to 1.6 mm x 2.7 mm x 100  $\mu\text{m}$  for the 11  $\mu\text{L}$  and 20  $\mu\text{L}$ ). Topographic scans for every experiment were processed in the same manner using the Profilm3D software. All profiles were first scale corrected and manually levelled, then invalid data points (surface points that were not detected by the profilometer) were interpolated using the “Fill In Invalids” tool. Topographical scans for each short-term bloodstain at each time point were taken after each processing step to produce a timelapse of the bloodstain over two hours, with a scale of 80  $\mu\text{m}$ .

### 2.4 Image Analysis and Data Processing

In Profilm3D, the ‘Area Roughness’ function was used to determine the surface average roughness, root mean square (RMS) roughness, skewness, and kurtosis of the entire bloodstain; the “Crop” function was used to remove as much of the aluminum plate as possible from the scans before analysis. The ‘Line Profile’ function was used to collect two height profiles from the bloodstain, one running from North to South (vertical slice), the other running East to West (horizontal slice), with both running through the centre of the bloodstain. Each bloodstain produced during the short-term experiments was also analyzed to determine the number of cracks present using FIJI (v. 2.30/1.53q). Like the long-term experiments, the “Area Roughness” function was used to determine the same surface characteristics and the maximum height of the bloodstain present within the scan. Surface average roughness was determined by calculating the average distance of surface points from the mean height plane [22]. The full, uncropped scans were exported as .txt files for analysis and figure conception in R Studio (V. 4.2.0). Pearson’s correlation coefficients ( $r$ ) were computed between pairs of surface characteristics to quantitatively evaluate their relationship.

To standardize the height profiles, the average height of the polished aluminum surface was recorded for each scan and subtracted from the maximum height in order to account for differences in surface height between time points. Heights were collected from overall bloodstains using horizontal and vertical slices, OriginPro (V. 9.7) was used to do a baseline subtraction to generate a corrected height profile. Points on the left and right of the bloodstain, as well as any cracks that reached the surface, were selected as anchor points. FIJI was used to analyze cracks and pits. After uploading the scans to FIJI and setting a scale, a colour threshold was created to only select surface colours. The image was converted to binary and subsequently cropped to remove the aluminum surface and any artefacts along the edge of the scan. The “Analyze Particles” function with a 8.5  $\mu\text{m}^2$  size filter was then used to measure the area of each crack and pit. It is important to note that the scans only surveyed a portion of the bloodstains; 5.52% for 4  $\mu\text{L}$ , 6.94% for 11  $\mu\text{L}$  and 4.77% for 20  $\mu\text{L}$  of the total stain area. A scaling factor of 1.2 and 1.3 was applied to the 4  $\mu\text{L}$  and 20  $\mu\text{L}$  respectively data for comparison.

### 3. Results

#### 3.1 Long-Term Experiment

In the long-term experiments, the bloodstain scans showed little variation between 1.5 hours and four weeks (Figure 1A). For the long-term experiments, kurtosis values showed slight variation over the four weeks (Supplemental S3), although the values were always less than three, indicating platykurtic distributions, or height profiles with multiple heights of similar frequencies. Skewness values showed similar timewise fluctuations but were influenced by individual bloodstain variation. For example, bloodstain 1 had overall negative skewness values, while bloodstains 2 and 3 had positive skewness values. Surface roughness slightly increased within the first day, but then plateaued over the tested timeframe. Maximum height was measured from the horizontal and vertical slices taken from the long-term bloodstains, where minimal change was observed in the height profile over time, except for the earlier time points (1.5 and 6 hours) which had lower heights at the centre of the bloodstain.

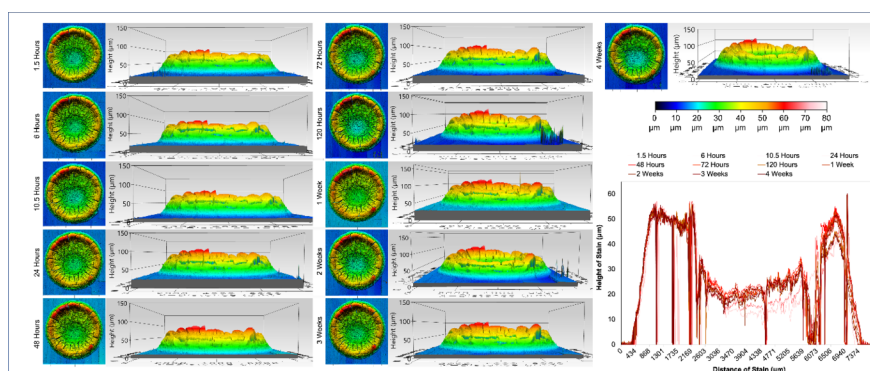


**Figure 1.** Topographical scans of the top and side of one 4  $\mu\text{L}$  bloodstain at varying times since deposition up to 4 weeks. The scans show the height ( $\mu\text{m}$ ) against the X-distance ( $\mu\text{m}$ ) on the plate. The corresponding height profile is taken from the vertical/horizontal slice of each scan over time is also shown (bottom right).

#### 3.2 Short-Term Experiment

Topographical scans for the short-term experiments indicate that in the first  $\sim 15$  minutes, the bloodstain changes from a liquid sessile drop to a soft-solid as more of the bloodstain can be detected by the profilometer (Figure 2). After the bloodstain had dried, the formation of the rim was observed, indicating that the majority of the RBCs had moved to the outside of the bloodstain (Figure 2, 15 minutes). The formation of cracks occurred between  $\sim 20$ -30 min, and after  $\sim 35$  minutes after deposition, there were no significant visual changes in the subsequent scans (Figure 2).

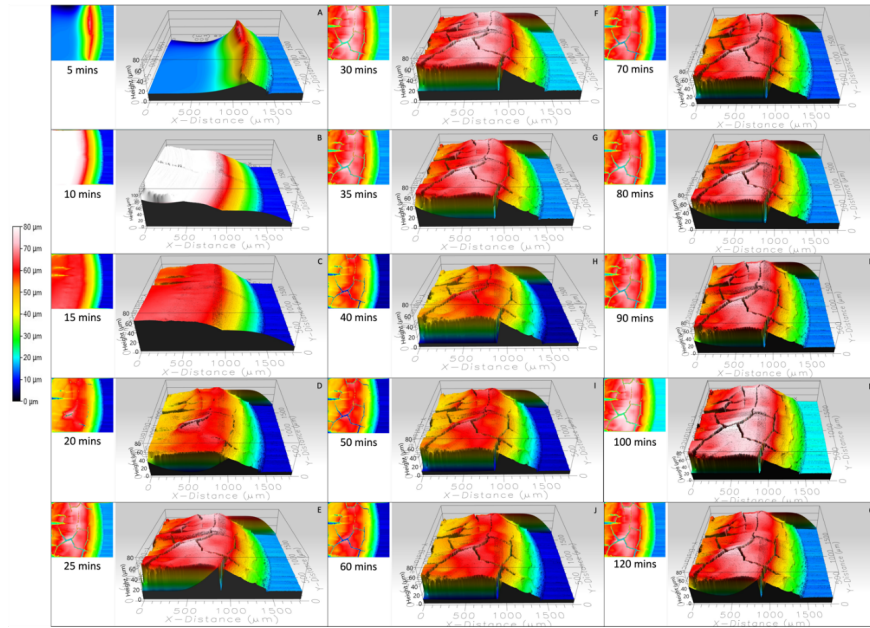


**Figure 2** . Topographical scans of the right side of a 4  $\mu\text{L}$  bloodstain. Scans were taken every 5 minutes after deposition up to 120 minutes. Scans of the 11  $\mu\text{L}$  and 20  $\mu\text{L}$  bloodstains can be found in Figures S1 and S2 of the supplemental.

A correlation matrix was used to assess the relationship between each surface characteristic in the short-term experiments. RMS roughness and surface roughness were found to be highly correlated ( $r = 0.99$ ). RMS roughness was also found to have a greater correlation with maximum height ( $r = 0.93$ ) compared to surface roughness ( $r = 0.89$ ); therefore, surface roughness was chosen for data interpretation. Some early data points were not included, as sections of the bloodstain were still liquid and could not be accurately measured by the profilometer, particularly in the larger blood volumes. Each volume of blood displayed similar general trends for each surface characteristic assessed, with differences between timepoints scalable to the volume of blood used (Figure 3).

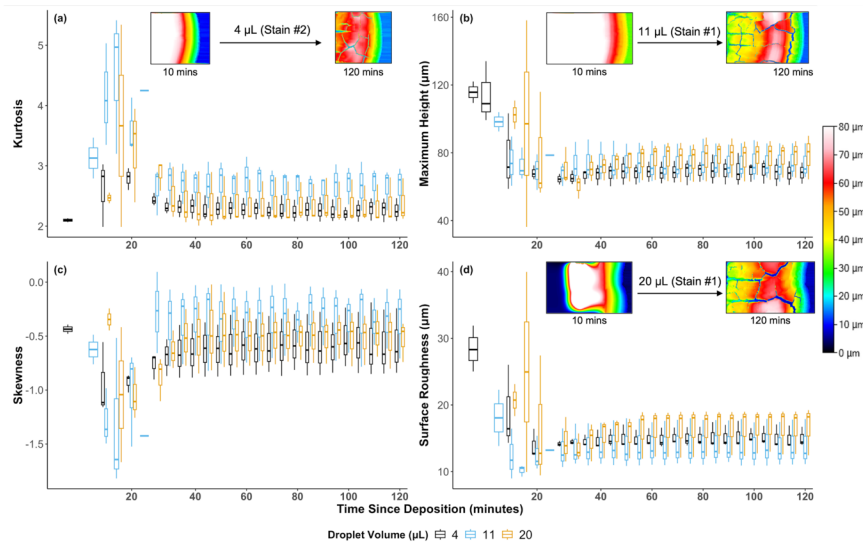


**Figure 3.** Average values ( $n=3$ ) for surface average roughness ( $\mu\text{m}$ ), maximum height ( $\mu\text{m}$ ), skewness, and kurtosis of the right side of degrading bloodstains of various volumes at varying time points after deposition. Inlet images show topographical scans from 4  $\mu\text{L}$  bloodstain (stain #2), 11  $\mu\text{L}$  bloodstain (stain #1) and 20  $\mu\text{L}$  bloodstain (stain #1) at 10 minutes and 120 minutes after deposition.

As the bloodstain desiccated, the surface average roughness decreased until approximately 20 minutes, and then increased slightly until plateauing at about 35-40 minutes (Figure 3, d). The maximum height of the bloodstains typically decreased until 20 minutes, which remained consistent until 120 minutes (Figure 3, b). A sharp decrease in height occurred as the bloodstain began to flatten out, and the rise around  $\sim 15$  minutes corresponded with the formation of the RBC ‘donut’ (Figure 3). This trend was more difficult to confirm in the larger volumes of blood due to the lack of time points prior to 10 minutes. Kurtosis increased until approximately 20 minutes, and also plateaued at about 40 minutes (Figure 3, a). Interestingly, 11  $\mu\text{L}$  displayed the greatest kurtosis values at almost every time point in the short-term experiments. The skewness values decreased up to 20 minutes, before increasing up to 40 minutes, where the values then plateaued (Figure 3, c). Similar to the kurtosis trends, the 11  $\mu\text{L}$  bloodstains had higher relative skewness values. Kurtosis and skewness displayed opposite trends within the first 40 minutes, which was corroborated by the correlation coefficient ( $r = -0.70$ ). Lastly, height distributions for the short-term experiments were assessed. The height of the bloodstain was higher at earlier time points and decreased sharply around 25-30 minutes (Figure 4). Interestingly, we observed variance in size distributions between volumes and replicates, with the maximum frequency ranging between approximately 30 – 60  $\mu\text{m}$ .

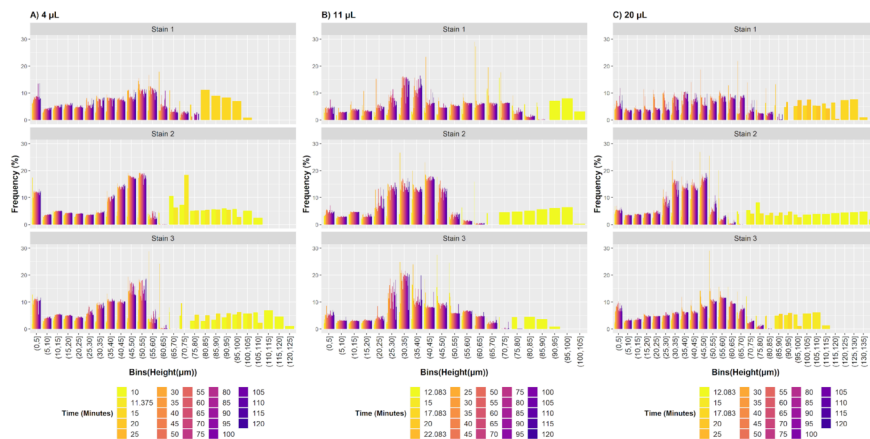


**Figure 4.** Height distribution from the right side of the degrading bloodstains at various timepoints (in minutes). The designated bin width was set to 5  $\mu\text{m}$ .

Additionally, we observe a high degree of variance in the number of observed cracks and pits; generally, for all stains, they increase rapidly for the first 30 minutes and then they plateau (Figure 5). Typical minute cracks around the edge of the bloodstain were not detected by the profilometer, making it difficult to assess when crack formation and propagation began, but it can be approximated to be  $\sim 15$ -20 minutes after deposition. Larger cracks located towards the centre of the bloodstain appeared around 20-25 minutes after deposition; surface average roughness values at these times slightly increased. Earlier time points also contained more cracks and pits with smaller areas which subsequently increased over time, leading to cracks with larger areas at later time points (Supplemental S4). There does not appear to be a volume dependence in this study as there is a high degree of variance observed in these data.

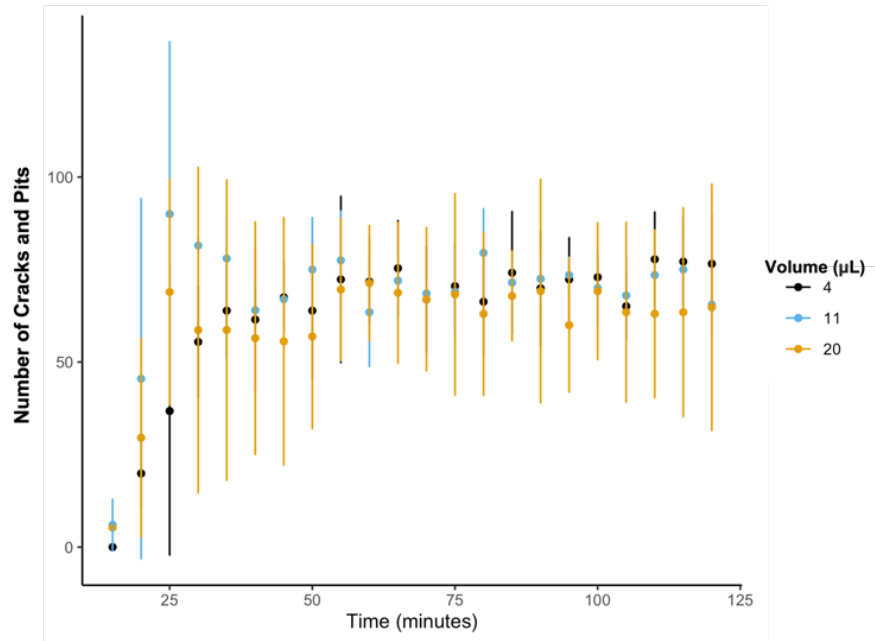


**Figure 5** . Total number of cracks and pits observed in the degrading bloodstains at various timepoints (in minutes).

#### 4. Discussion

Overall, our findings corroborate and are supported by the literature on bloodstain drying, suggesting that optical profilometry is a viable technique to observe and characterize bloodstain drying and degradation. In the short-term experiments, scans showed significant changes within the first 35-40 minutes after deposition, after which the surface characteristics plateaued. The pre-gelation phase begins as soon as the droplet is deposited onto the plate, however, many of the surface characteristics could not be obtained immediately due to the liquid-state of the bloodstain. Topographical scans could detect the edge of bloodstains five minutes after deposition, signifying the beginning of drying. Within the first 15-20 minutes of drying, height profiles and maximum height observations showed a significant change, with differences as large as 60  $\mu\text{m}$  within a 10-minute timespan. The change(s) in surface roughness, skewness, kurtosis and maximum height of the bloodstain over time is primarily driven by RBC movement [10,23]. As the RBCs gather along the edge of the bloodstain to form the rim, the maximum height will increase and the skewness and kurtosis values will change. The height distributions corroborate this and show that there is a decrease, then an increase in overall height as the rim of the bloodstain begins to form. The surface average roughness values could be correlated to RBC movement during drying. At earlier time points (before 20 minutes), the bloodstains contained no cracks, and the maximum height was in the centre of the bloodstain (Figure 2). As the RBCs moved towards the outside of the bloodstain and the surface temporarily flattened out, the surface average roughness value decreased. Then, as the rim began to form, the surface average roughness increased and cracks and pits formed. Cracks continued to form until  $\sim 30$ -35 minutes after deposition; all surface characteristics and height profile data then displayed a plateau, suggesting that no further changes occurred. The analysis of the area of cracks and pits over time was completed as a quantitative complement to the qualitative observations made using the topographical scans. Importantly, the profilometer will not interpolate a crack or pit. If a crack is present, but only one surface point is detected, it might interpolate the crack as much smaller than it is and, in some cases, it might only appear as one pixel after the scan is interpolated. This means that some cracks are larger than what the analysis determined; however, we decided rather than focus on the absolute value of a single crack/pit, the trend in the size of cracks and pits over time is more relevant. Similar to our work, Brutin et al. (2011) [23] found the drying time of approximately 10  $\mu\text{L}$  of human blood to be 36

minutes (temperature = 22 °C), while Ramsthaller et al. [8] found the drying time of ~25 µL of human blood to be 34 minutes (temperature = 24 °C). Although outside the scope of this study, these findings suggest that different blood sources (bovine vs. human) display comparable drying mechanisms. The inclusion of an anticoagulant also can account for differences in drying time.

From an imaging and spectroscopy perspective, it is important to understand the surface profiles of bloodstains for TSD estimates. Where the light source is focused could have spectral implications – for example, unwanted scattering. Having an idea of surface roughness changes and cracks and pits formation over time may help explain observed spectral variance beyond inter- and intra-specific variation between bloodstain samples. While there is a significant effect of spectral signatures with time, the variation between TSD models is also high due to substrate-dependent interactions and environmental effects. However, given the large observed variance in surface topography of the dried bloodstain, we wonder how much this also influences models, particularly those that use solid-state imaging techniques.

## 5. Conclusion

Optical profilometry provided detailed topographical scans of degrading whole bloodstains, an area not yet explored in the forensic literature. We were able to characterize the drying of three different bloodstain volumes through the analysis of relevant surface characteristics. Importantly, this work investigated the timewise degradation of whole blood, expanding on previous work that explored the drying of blood and other biocolloidal fluids. Using this method, we observed that most of the timewise changes to drying bloodstains occur within the first 35 minutes after deposition. Over a longer time period, the overall surface morphology shows little variation, currently limiting the use of optical profilometry as a standalone technique in TSD estimates. Optical profilometry has previously been paired with SEM [24] and AFM [25] for imaging purposes; combining these two techniques could be useful for a more detailed analysis of crack and pit formation. In addition, factors such as viscosity, temperature, PCV%, and blood diseases affect the drying of bloodstains [8,9,11,26]. Further research into these factors should be undertaken to understand their effects on the topography of degrading bloodstains [8,9,11,26]. Additionally, the influence of topography on spectral changes for TSD estimation should also be considered. Finally, various substrates, such as those with rougher surfaces, may lead to interesting crack formation and timewise trends with bloodstain degradation that could be captured using optical profilometry.

## 6. References

1. James SH, Kish PE, Sutton TP. Introduction to Bloodstain Pattern Analysis. In: Principles of Bloodstain Pattern Analysis: Theory and Practice. Boca Raton, Florida: CRC Press, 1985;1–10..
2. Pagliaro E. Blood and physiological fluid evidence. In: Harris H, Lee HC, editors. Introduction to Forensic Science and Criminalistics. Boca Raton, Florida: CRC Press, 2019;223–53.
3. James SH, Kish PE, Sutton TP. Biological and physical properties of human blood. Principles of Bloodstain Pattern Analysis: Theory and Practice. Boca Raton: CRC Press, 2005;41–57.
4. Chhabra RP. Non-Newtonian fluids: An introduction. In: Krishnan J, Deshpande A, Kumar P, editors. Rheology of Complex Fluids. New York: Springer, 2010;3–34.
5. Zadora G, Menzyk A. In the pursuit of the holy grail of forensic science – Spectroscopic studies on the estimation of time since deposition of bloodstains. Trends Anal Chem 2018;105(5):137–65. <https://doi.org/10.1016/j.trac.2018.04.009>.
6. Benabdelhalim H, Brutin D. Phase separation during blood spreading. Sci Rep 2021;11:1–13. <https://doi.org/10.1038/s41598-021-90954-5>.
7. Laan N, Smith F, Nicloux C, Brutin D. Morphology of drying blood pools. Forensic Sci Int 2016;267:104–9. <https://doi.org/10.1016/j.forsciint.2016.08.005>

8. Ramsthaler F, Schmidt P, Bux R, Potente S, Kaiser C, Kettner M. Drying properties of bloodstains on common indoor surfaces. *Int J Legal Med* 2012;126:739–46. <https://doi.org/10.1007/s00414-012-0734-2>.
9. Larkin BAJ, Banks CE. Exploring the effect of specific packed cell volume upon bloodstain pattern analysis: blood drying and dry volume estimation. *Can Soc Forensic Sci J* 2015;48(4):167–89. <https://doi.org/10.1080/00085030.2015.1083161>.
10. Sobac B, Brutin D. Desiccation of a sessile drop of blood: Cracks, folds formation and delamination. *Colloids Surfaces A Physicochem Eng Asp* 2014;448:34–44. <https://doi.org/10.1016/j.colsurfa.2014.01.076>.
11. Zeid WB, Brutin D. Influence of relative humidity on spreading, pattern formation and adhesion of a drying drop of whole blood. *Colloids Surfaces A Physicochem Eng* 2013;430:1–7. <https://doi.org/10.1016/j.colsurfa.2013.03.019>.
12. Pal A, Gope A, Iannacchione G. Temperature and concentration dependence of human whole blood and protein drying droplets. *Biomolecules* 2021;11(2):1–18. <https://doi.org/10.3390/biom11020231>.
13. Hortolà P. SEM analysis of red blood cells in aged human bloodstains. *Forensic Sci Int* 1992;55:139–59.
14. Wu Y, Hu Y, Cai J, Ma S, Wang X, Chen Y, et al. Time-dependent surface adhesive force and morphology of RBC measured by AFM. *Micron* 2009;40(3):359–64. <https://doi.org/10.1016/j.micron.2008.10.003>.
15. Cavalcanti DR, Silva LP. Application of atomic force microscopy in the analysis of time since deposition (TSD) of red blood cells in bloodstains: A forensic analysis. *Forensic Sci Int* 2019;301:254–62. <https://doi.org/10.1016/j.forsciint.2019.05.048>.
16. Edelman G, van Leeuwen TG, Aalders MCG. Hyperspectral imaging for the age estimation of blood stains at the crime scene. *Forensic Sci Int* 2012;223:72–7. <https://doi.org/10.1016/j.forsciint.2012.08.003>.
17. Majda A, Wietecha-Posłuszny R, Mendys A, Wójtowicz A, Lydzba-Kopczyńska B. Hyperspectral imaging and multivariate analysis in the dried blood spots investigations. *Appl Phys A Mater Sci Process* 2018;124(4):1–8. <https://doi.org/10.1007/s00339-018-1739-6>.
18. Schmit J, Creath K, Wyant J. Surface profilers, Multiple Wavelength, and White Light Interferometry. In: Malacara D, editor. *Optical Shop Testing*. Hoboken, New Jersey: John Wiley & Sons, Inc, 2007;674–764.
19. Alcaraz-fossoul JD, Mancenido M, Soignard E. Application of 3D imaging technology to latent fingerprinting studies. *J Forensic Sci* 2019;64(2):570–6. <https://doi.org/10.1111/1556-4029.13891>.
20. Heikkinen V, Kassamakov I, Hægström E. Scanning White Light Interferometry, -a new 3D forensics tool. *IEEE International Conference on Technologies for Homeland Security (HST)*. 2011;332–7.
21. Hertaeg MJ, Tabor RF, Routh AF, Garnier G, Routh AF, Garnier G. Pattern formation in drying blood drops. *Philos Trans A* 2021;379. <https://doi.org/10.1098/rsta.2020.0391>.
22. Filmetrics. *Profilm optical profiling software: Profilm user manual*. 2018.
23. Brutin D, Sobac B, Loquet B, Sampol J. Pattern formation in drying drops of blood. *J Fluid Mech* 2011;667:85–95. <https://doi.org/10.1017/S0022112010005070>.
24. Daud A, Gray G, Lynch CD, Wilson NHF, Blum IR. A randomised controlled study on the use of finishing and polishing systems on different resin composites using 3D contact optical profilometry and scanning electron microscopy. *J Dent* 2018;71:25–30. <https://doi.org/10.1016/j.jdent.2018.01.008>.
25. Fischer NG, Dang J, Takamizawa T, Tsujimoto A, Barkmeier WW, Baruth AG. The role of spatial frequency analysis in correlating atomic force microscopy and optical profilometry with self-etch adhesive enamel bond fatigue durability. *Microsc Res Tech* 2019;82:1419–29. <https://doi.org/10.1002/jemt.23294>.
26. Bahmani L, Neysari M, Maleki M. The study of drying and pattern formation of whole human blood drops and the effect of thalassaemia and neonatal jaundice on the patterns. *Colloids Surfaces A Physicochem*

